IJISEM
INTERNATIONAL JOURNAL OF INNOVATIONS IN SCIENCE ENGINEERING AND MANAGEMENT

International Journal of Innovations In Science Engineering And Management

OPEN ACCESS

Volume: 4

Issue: 2

Month: May

Year: 2025

ISSN: 2583-7117

Published: 30.05.2025

Citation:

Rajni Kant Verma, Ashok Jangid, Ranjit Kumar "Tunable Gas Sensing Properties of ZnO Thin Films through Layer Engineering: Structural, Morphological, and Optical Analysis" International Journal of Innovations in Science Engineering and Management, vol. 4, no. 2, 2025, pp. 230–237.

DOI:

10.69968/ijisem.2025v4i2230-237

Tunable Gas Sensing Properties of ZnO Thin Films through Layer Engineering: Structural, Morphological, and Optical Analysis

Rajni Kant Verma[1], Ashok Jangid[2], Ranjit Kumar[3]

[1]Department of Physics and Computer Science, Dayalbagh Educational Institute, (Deemed to be University), Dayalbagh, Agra.
[2]Department of Physics and Computer Science, Dayalbagh Educational Institute, (Deemed to be University), Dayalbagh, Agra.
[3]Department of Chemistry, Dayalbagh Educational Institute, (Deemed to be University), Dayalbagh, Agra.

Abstract

The sol-gel method was employed to effectively "synthesise multilayer ZnO thin films with 3, 5, and 7 layers". The films were characterised for their optical, compositional, morphological, and structural properties. The crystalline quality was enhanced, as evidenced by the decrease in dislocation density and the increase in crystallite size as the number of layers increased, as confirmed by X-ray diffraction (XRD) and "the hexagonal wurtzite structure with a preferential (002) orientation". Field Emission Scanning Electron Microscopy (FESEM) revealed uniform and granular surface morphology, consistent across all layers, with particle size increasing slightly in thicker films. Energy Dispersive Spectroscopy (EDS) validated nearly stoichiometric Zn and O composition, with no significant variation due to the number of layers, indicating high purity. UV-Vis spectroscopy demonstrated strong UV absorption and excellent transparency in the visible region, with optical bandgap values of 2.66 eV, 2.80 eV and 2.81 eV for 3, 5 and 7 layers, respectively, suggesting improved optical properties in thicker films. The results confirm the suitability of these films for optoelectronic, UV-sensing, and photocatalytic applications, with tunable properties enabled by varying the number of layers. This study underscores the reliability of the sol-gel method for fabricating high-quality multilayer ZnO thin films.

Keywords; Multilayer, Semiconductor, Gas Sensing, ZnO, XRD, FESEM, UV-vis.

INTRODUCTION

Zinc oxide is an exceptionally attractive material, offering a distinct set of advantages like non-toxicity, widespread availability, cost-effectiveness, and a substantial direct bandgap of 3.2–3.4 eV typical of II-VI semiconductors (Kuddus et al., 2024; Salim & Amroun, 2022). Furthermore, it is vital for a variety of applications, including gas sensing and solid-state optoelectronic devices, among others. ZnO demonstrates remarkable gas-sensing capabilities to its high surface area, excellent chemical stability, and ability to interact with gas molecules at its surface (Borysiewicz, 2019; Raub et al., 2024; Shahzad et al., 2021). As a wide-bandgap semiconductor, its gas-sensing performance is largely determined by surface adsorption and desorption processes that influence its electrical conductivity (Pearton et al., 2010; Xuan et al., 2020). Due to its exceptional optical, morphological, and structural characteristics, ZnO is considered highly appropriate for a variety of gas sensing applications (Leonardi, 2017). This study highlights the potential of multilayered ZnO thin films for enhanced gas sensing, identifies a research gap in the exploration of their properties when synthesized via the cost-effective sol-gel technique, and aims to advance affordable gas sensing devices by systematically examining the structural, morphological, and optical properties of three, five, and seven-layer ZnO thin films fabricated using the sol-gel spin coating method.

Experimental details

The multilayer ZnO thin films were fabricated using the sol-gel method. 20 millilitres of 2-methoxyethanol were used to dissolve 0.60 grammes of "zinc acetate dihydrate" in order to create the ZnO solution. After an hour at 80°C, the solution was agitated using a magnetic stirrer. The mixture was subsequently agitated at 60°C for a period of 90 minutes after the addition of glycerol as a stabiliser. A clear, uniform ZnO solution was obtained by ageing the mixture for a full day. Film deposition was feasible after the solution was made available. The glass substrate was placed in the spin coating system, with the rotation speed set to 3000 rpm for 30 seconds per sample. Drops of the sol-gel solution were applied to the glass substrate according to the required number of layers. After 30 seconds, the substrate was removed from the spin coater and placed on a hot plate to dry at 100°C for about 10 minutes. This process was repeated to create multiple thin layers. A muffle furnace was used to transmit the thin coatings, and the temperature was progressively raised to 350°C. Upon attaining the desired temperature, the furnace was deactivated and the samples were permitted to settle to ambient temperature. The samples were prepared for analysis after chilling.

Characterization Techniques Used

Several analytical methods were used to characterise the produced thin films: Data was gathered at a scan rate of 2 seconds per step across a 2θ range of 20° to 80° using X-ray diffraction (XRD) using "a Bruker AXS D8 Advance diffractometer and Cu Kα radiation (wavelength 1.5406 Å)" to investigate the crystal structure and phase composition. The bandgap in the UV-Vis region was ascertained and absorption characteristics were investigated using ultraviolet-visible (UV-Vis) spectroscopy. Surface morphology was investigated using a JEOL JSM-7610F Plus SEM for "Field Emission Scanning Electron Microscopy (FESEM)", and particle size distributions were evaluated using ImageJ software. Energy Dispersive X-ray (EDAX) was employed to analyse the elemental composition using a Peltier-cooled Octane Plus system. This system has a 30 mm² detector area and a resolution of 127 eV.

RESULTS AND DISCUSSION

XRD Analysis of ZnO Thin Films

The ZnO thin film's diffraction pattern is shown in "the XRD (X-Ray Diffraction)" picture in **Figure *1***, which offers information on the phase composition, orientation, and crystallographic structure of the material. The x-axis represents the 2θ values (diffraction angles), while the y-axis denotes intensity in arbitrary units (a.u.). Peaks in the pattern correspond to specific planes of the ZnO crystal lattice that satisfy Bragg's Law. ZnO typically crystallizes in a hexagonal wurtzite structure, with characteristic peaks observed at specific 2θ values, such as 31.7° at the (100) plane, 34.4° at the (002) plane, and 36.2° at the (101) plane. Additional smaller peaks may correspond to other planes like (102), (110), (103), and so on. These peak positions should be confirmed using the JCPDS reference card (36-1451) to validate the presence of the wurtzite ZnO phase. Higher peak intensities typically indicate better crystallinity of the thin films. The information derived from this pattern can be used to assess the quality and structural attributes of the synthesized ZnO thin films (Salim & Azzaoui, 2023).

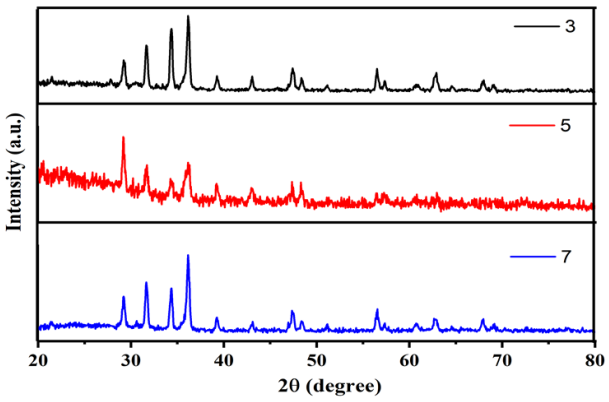

Figure 1 XRD Pattern of Multilayer ZnO three, five, and seven-layer thin film

Table 1 XRD summary of three-layer, five layer and Seven-layer ZnO thin films.

Sr. No.	Peak Position (2θ)	hkl	d-spacing Å	FWHM (radians)	Crystallites size (nm)	Phase	Dislocation density x 10^{14} m^{-2}
1.	31.7	100	2.816	0.0032	45	ZnO	4.94
2.	34.4	002	2.601	0.0028	50	ZnO	4
3.	36.2	101	2.480	0.0036	40	ZnO	6.25
4.	47.5	102	1.914	0.0042	35	ZnO	8.16
5.	56.6	110	1.625	0.0038	38	ZnO	6.93

XRD- d-spacing calculation

Bragg's law is the source of the formula utilised to determine the d-spacing:

$$n\lambda = 2dsin \quad (1)$$

The formula becomes simpler for the first order diffraction (n=1) to

$$d = \frac{\lambda}{2sin\theta} \quad (2)$$

Where, d = interplanar spacing (Å), λ = 1.5406Å (Wavelength of Cu-Kα radiation), θ = 2θ/2 = Bragg angle in radians (half of the 2θ value), Sinθ = sine of the Bragg angle

XRD – Grain size calculation

The Crystallites size is calculated by the using the Scherrer equation:

$$D = \frac{K\lambda}{\beta cos\theta} \quad (3)$$

Where D is the size of the crystallite (in nanometres), K is the shape factor (usually considered to be 0.9), λ is the X-ray wavelength (1.5406 Å for Cu-K/a), and β is "the full width of half maximum (FWHM) in radians". Θ is the Bragg angle, which is equal to half of the two θ values in radians. For multilayer ZnO thin films, the computed particle sizes for "2θ values of 31.7o, 34.4o, 36.2o, 47.5o, and 56.6o are 45 nm, 50 nm, 40 nm, 35 nm, and 38 nm each".

XRD – Dislocation density

A material's dislocation density is a measurement of the quantity of dislocations, or crystal lattice defects, per unit volume. It is an important parameter in material science because it provides insights into the quality strength and mechanical behaviour of a crystalline material (Ni et al., 2012). The following relation is used to compute the dislocation density:

$$\sigma = \frac{1}{D^2} \quad (4)$$

Where, σ = Dislocation density (in m-2) and D = Crystallite size (in nm). A higher dislocation density indicates a larger number of defects in the crystal structure, meaning the material is more imperfect and lower dislocation density suggests fewer defects and better crystalline quality of material. The dislocation line density of multilayer thin films at "2θ values of 31.7o, 34.4o, 36.2o, 47.5o and 56.6o"are 4.94 x 1014 m-2, 4 x 1014 m-2, 6.25 x 1014 m-2, 8.16 x 1014 m-2, and 6.93 x 1014 m-2, respectively.

FESEM results

The FESEM micrographs presented in **Figure *2*** depict the surface morphology of three-layer, five-layer, and seven-layer ZnO thin films. All samples exhibit a similar granular structure with uniformly distributed nanocrystals, indicating a consistent and high-quality deposition process likely achieved using the sol-gel technique (Kasar et al., 2016). This uniform morphology across all samples suggests that the increase in the number of layers does not significantly impact the surface structure or grain distribution. The layer-by-layer growth appears to be well-controlled, ensuring the absence of additional defects or irregularities as the number of layers increases. This finding supports the sol-gel technique's dependability in creating superior ZnO thin films with consistent surface characteristics.

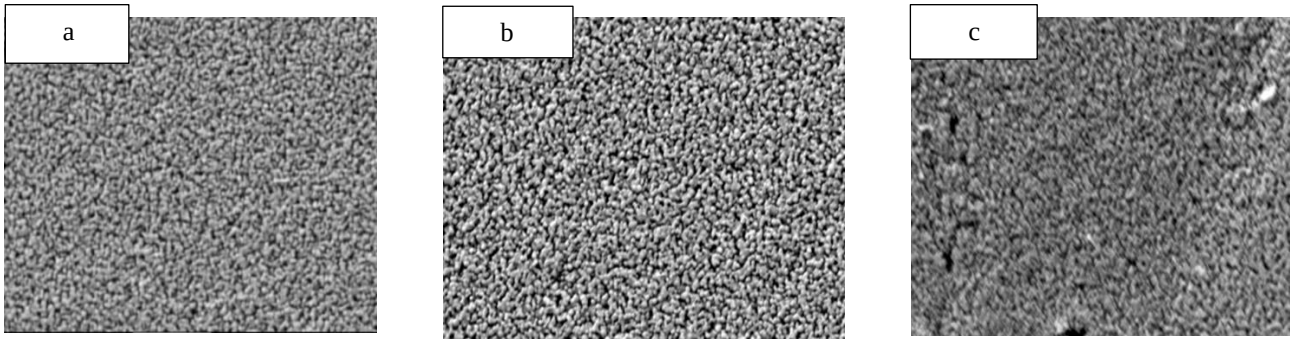

Figure 2 FESEM Micrographs of (a) three layer (b) Five layer (c) Seven-layer ZnO thin film

This similarity across different layers may also reflects the saturation of grain growth beyond a certain thickness, with grain size and texture stabilizing as additional layer are deposited. Such stability in surface morphology across multilayer films is advantageous for maintain uniformity in optical, electronic, and mechanical properties, which are critical for applications in device like sensors, photovoltaics and optoelectronic components. The FESEM result confirm that the layer variation does not compromise the structural

quality of the films, underscoring the reliability and reproducibility of the synthesis process.

EDS Results

EDS Analysis of ZnO Thin Films

The EDS (Energy Dispersive Spectroscopy) results, presented in **Figure *3***, provide elemental composition data for the multilayer ZnO thin films, confirming the successful fabrication and stoichiometry of the material (Abou-Ras et al., 2011). The EDS spectrum and quantitative analysis reveal that zinc (Zn) and oxygen (O) are the primary constituents, with zinc accounting for 78.38 atomic % and oxygen for 24.62 atomic %. Their respective weight percentages are 42.90% and 57.10%. These results align closely with the expected stoichiometry of ZnO, ensuring that the material's composition is appropriate for its intended applications. The study validates the high calibre of the synthesised ZnO thin films and the accuracy of the production method.

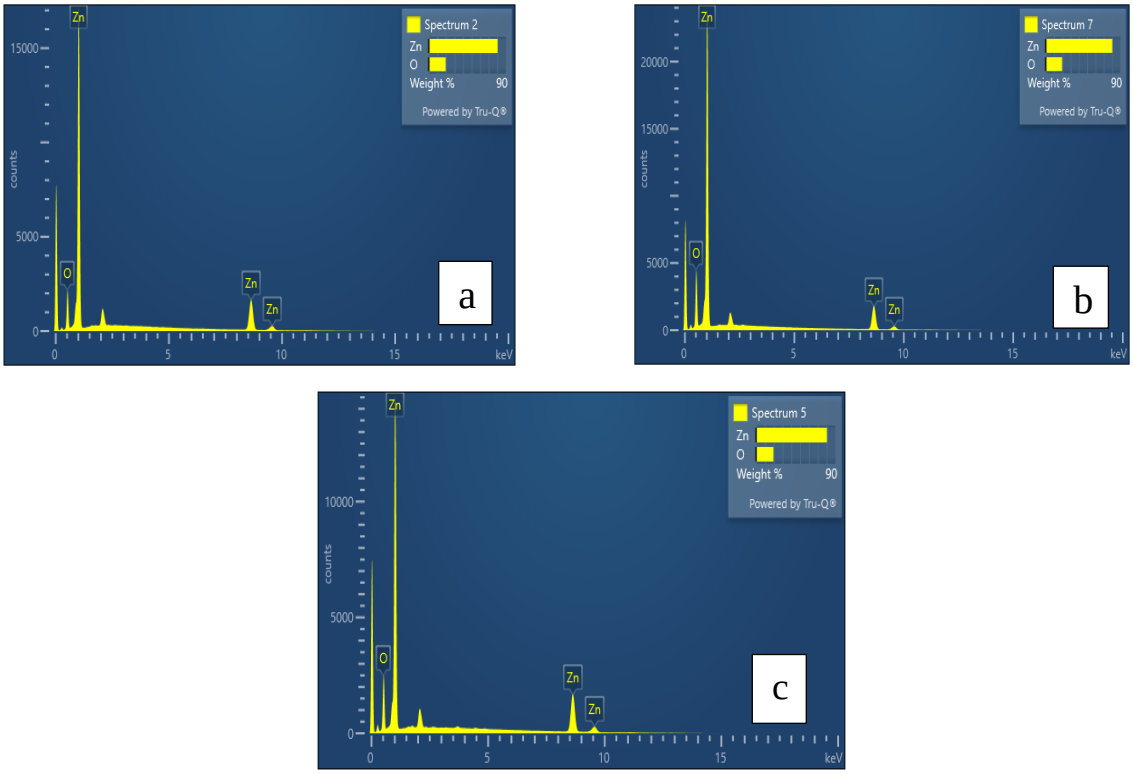

Figure 3 EDS Spectra image of (a) three layer (b) Five layer (c) Seven-layer ZnO thin films

The slight deviation from ideal stoichiometry could arise from oxygen vacancies or zinc interstitials, common in ZnO, which can influence its electronic and optical properties. These properties, combined with the verified elemental purity, confirm the suitability of multilayer ZnO thin film for application in optoelectronics, sensors, and photocatalysis. The results demonstrate that the multilayer fabrication process does not compromise the chemical integrity of the films, supporting their use in advanced material applications.

Optical Properties

UV-Vis Absorption Spectra of ZnO Thin Films

Figure *4* displays "the UV-Vis absorption spectra", which demonstrate the optical characteristics of ZnO thin films with three, five, and seven layers. Strong UV absorption (below 400 nm) is seen in all of the films, which is consistent with electronic transitions close to ZnO's optical bandgap. The absorption dramatically drops in the visible range (400–800 nm), suggesting great transparency to visible light (Samadi et al., 2016). As the number of layers increases, the overall absorption in the UV region also increases, suggesting that thicker films possess higher optical density, leading to more significant photon absorption. These findings underscore the significance of film thickness in determining the optical properties of ZnO thin films, which is essential for customising "their performance in optoelectronic applications".

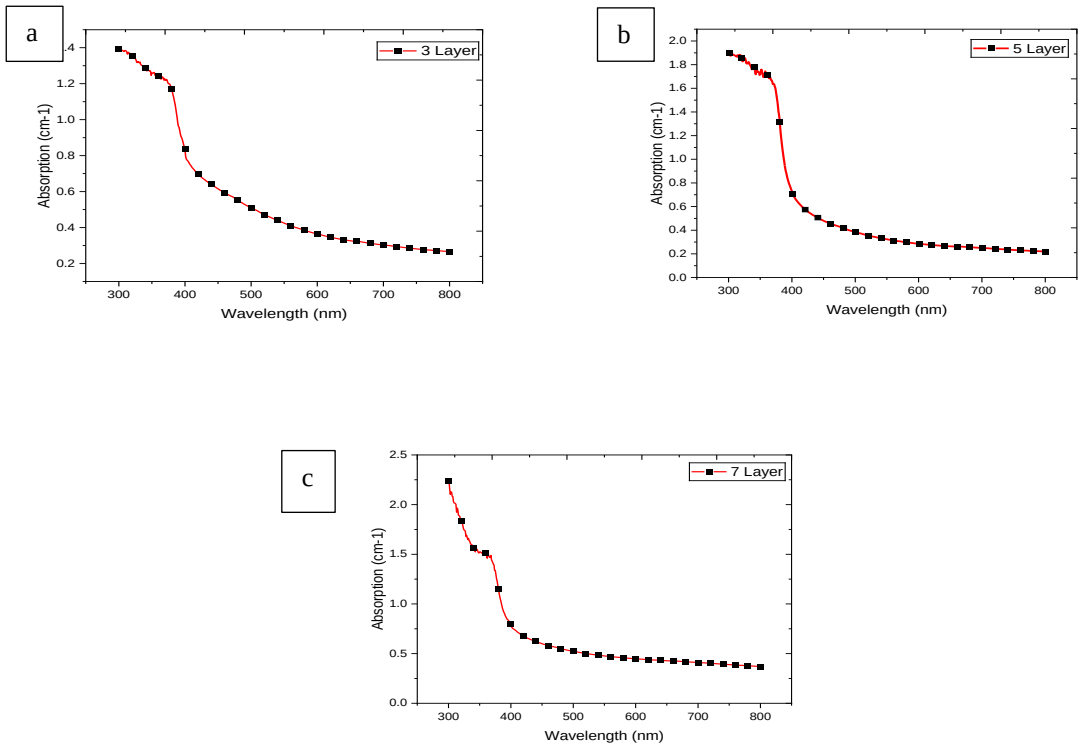

Figure 4 Absorption spectra of (a) three layer (b) Five layer (c) Seven-layer ZnO thin films

The number of layers has a significant impact on the optical characteristics of ZnO thin films, as seen by the UV-Vis absorption spectra, with thicker films showing better absorption and crystallinity. These characteristics make the films highly suitable for a wide range of optical and electronic application.

UV-Vis Transmittance Spectra of ZnO Thin Films

The UV-Vis transmittance spectra, displayed in **Figure *5***, demonstrate the optical behaviour of three-layer, five-layer, and seven-layer ZnO thin films. All films exhibit low transmittance in the UV region (300–400 nm), corresponding to strong absorption by ZnO. This behaviour is attributed to electronic transitions near the bandgap energy, where photons with sufficient energy are absorbed. All films exhibit a considerable improvement in transmittance in the visible band (400–800 nm), demonstrating high optical transparency (Ren et al., 2022). This characteristic is essential for use in optoelectronic technologies and transparent conductive devices. The overall transmittance experiences a minor decrease as the quantity of layers increases, which is a result of the films' increased thickness (Zhang et al., 2014). Thicker films enhance light absorption and scattering within the material, leading to a modest reduction in transparency (Gao et al., 2016).

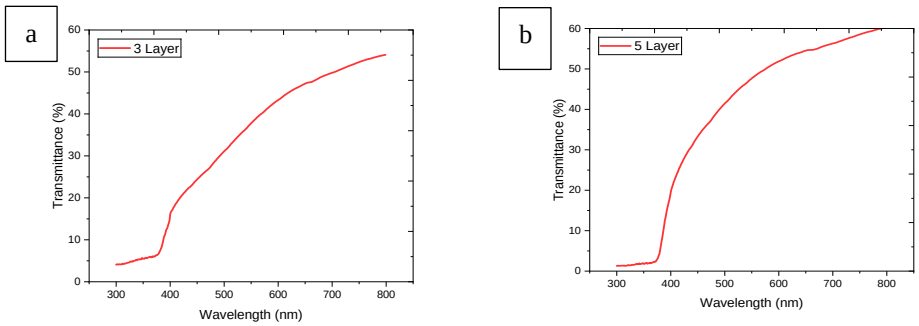

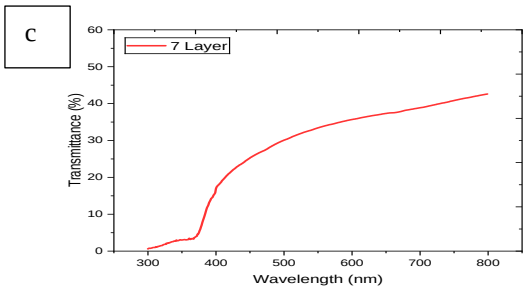

Figure 5 Transmittance spectra of (a) three layer (b) Five layer (c) Seven-layer ZnO thin films

Optical Bandgap Determination of ZnO Thin Films

The UV-Vis analysis of the three-layer, five-layer, and seven-layer ZnO thin films, as presented in **Figure *6***, reveals variations in their optical bandgap energy, determined using Tauc plots. The Tauc plot formula is given by (Klein et al., 2023)

$$(\alpha hv)^n = A(hv - Eg) \qquad (5)$$

Where n depends on the kind of "electronic transition (for ZnO, n=2, indicating a direct permitted transition)", absorption coefficient α, photon energy hv, optical bandgap energy Eg, and constant A (Kaushal & Kaur, 2011). The three-layer film exhibits the lowest bandgap of 2.66 eV, likely due to higher defect densities, such as oxygen vacancies or zinc interstitials, or lower crystalline quality compared to thicker films. The five-layer film shows an intermediate bandgap of 2.80 eV, indicating improved crystallinity and reduced defects with additional layers. The seven-layer film demonstrates the highest bandgap of 2.81 eV, suggesting that the optical properties stabilize as the number of layers increases, with minimal further reduction in structural defects (Li et al., 2015).

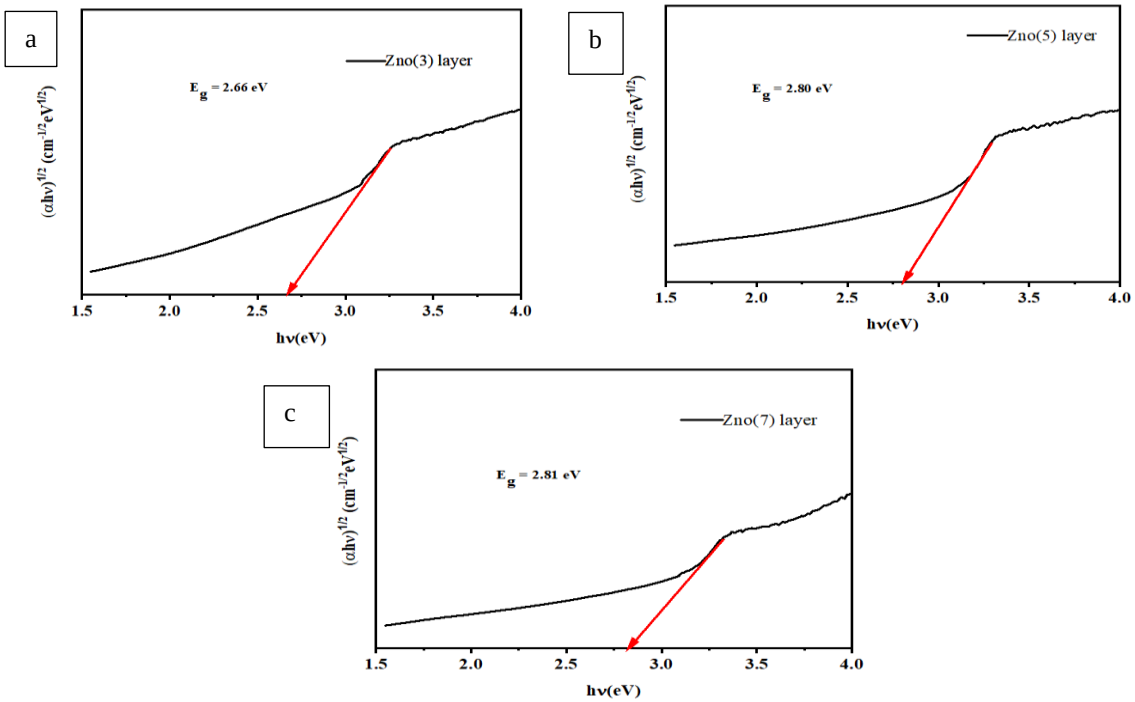

Figure 6 Optical band gap of (a) three layer (b) Five layer (c) Seven-layer ZnO thin films

Layer thickness's impact on optical and electronic properties is underscored by the modest variation in bandgap observed in the films. All films exhibit bandgaps lower than the bulk ZnO bandgap (3.37 eV), which can be attributed to structural defects or quantum size effects. These properties make the films suitable for optoelectronic applications, particularly in UV-sensitive devices. Moreover, the consistency in bandgap values with increasing layers demonstrates the uniformity and reliability of the multilayer deposition process.

CONCLUSION

Their suitability for gas sensing applications is demonstrated by the structural, morphological, compositional, and optical characterisation of "multilayer ZnO thin films (three, five, and seven layers)". "Gas adsorption and surface reactivity" depend on the hexagonal wurtzite structure's strong c-axis alignment and dominating (002) orientation, which XRD verified. The increasing crystallite size and decreasing dislocation density with more layers indicate improved crystallinity, which enhances the stability and sensitivity of the material for gas detection. FESEM images revealed a uniform, granular surface morphology across all layers, with a slight increase in particle size for thicker films. This uniform surface and well-distributed nanostructures provide a high surface area, promoting efficient interaction with gas molecules. EDS analysis verified nearly stoichiometric Zn and O compositions with minimal contamination, ensuring chemical stability and reliability in gas sensing environments. "For three, five, and seven layers", the bandgap values were 2.66 eV, 2.80 eV, and 2.81 eV, respectively, indicating good transparency in the visible range and substantial UV absorption. Through electronic transitions close to the bandgap, these figures show how thickness affects electrical and optical characteristics, which in turn affect how sensitive the films are to gas adsorption. The combination of excellent structural, morphological, and optical properties, along with the tunability of layer thickness, confirms that these ZnO thin films are highly suitable for gas sensing applications. The enhanced surface area, stability, and tailored optical properties make them ideal for detecting a range of gases with high sensitivity and selectivity.

REFERENCES

[1] Abou-Ras, D., Caballero, R., Fischer, C.-H., Kaufmann, C. A., Lauermann, I., Mainz, R., Mönig, H., Schöpke, A., Stephan, C., & Streeck, C. (2011). Comprehensive comparison of various techniques for the analysis of elemental distributions in thin films. Microscopy and Microanalysis, 17(5), 728–751.

[2] Borysiewicz, M. A. (2019). ZnO as a functional material, a review. Crystals, 9(10).

[3] Gao, J., Kempa, K., Giersig, M., Akinoglu, E. M., Han, B., & Li, R. (2016). Physics of transparent conductors. Advances in Physics, 65(6), 553–617.

[4] Kasar, C. K., Sonawane, U. S., Bange, J. P., & Patil, D. S. (2016). Optical and structural properties of nanoscale undoped and cerium doped ZnO with granular morphology. Journal of Materials Science: Materials in Electronics, 27, 11885–11889.

[5] Kaushal, A., & Kaur, D. (2011). Pulsed laser deposition of transparent ZnO/MgO multilayers. Journal of Alloys and Compounds, 509(2), 200–205.

[6] Klein, J., Kampermann, L., Mockenhaupt, B., Behrens, M., Strunk, J., & Bacher, G. (2023). Limitations of the Tauc plot method. Advanced Functional Materials, 33(47), 2304523.

[7] Kuddus, A., Mostaque, S. K., Mouri, S., & Hossain, J. (2024). Emerging II-VI wide bandgap semiconductor device technologies. Physica Scripta, 99(2), 022001.

[8] Leonardi, S. G. (2017). Two-dimensional zinc oxide nanostructures for gas sensor applications. Chemosensors, 5(2), 17.

[9] Li, X., Zhang, F., & Zhao, D. (2015). Lab on upconversion nanoparticles: optical properties and applications engineering via designed nanostructure. Chemical Society Reviews, 44(6), 1346–1378.

[10] Ni, S., Wang, Y. B., Liao, X. Z., Figueiredo, R. B., Li, H. Q., Ringer, S. P., Langdon, T. G., & Zhu, Y. T. (2012). The effect of dislocation density on the interactions between dislocations and twin boundaries in nanocrystalline materials. Acta Materialia, 60(6–7), 3181–3189.

[11] Pearton, S. J., Ren, F., Wang, Y.-L., Chu, B. H., Chen, K. H., Chang, C. Y., Lim, W., Lin, J., & Norton, D. P. (2010). Recent advances in wide bandgap semiconductor biological and gas sensors. Progress in Materials Science, 55(1), 1–59.

[12] Raub, A. A. M., Bahru, R., Nashruddin, S. N. A. M., & Yunas, J. (2024). A review on vertical aligned zinc oxide nanorods: Synthesis methods, properties, and applications. Journal of Nanoparticle Research, 26(8), 186.

[13] Ren, Y., Liu, P., Liu, R., Wang, Y., Wei, Y., Jin, L., & Zhao, G. (2022). The key of ITO films with high transparency and conductivity: Grain size and

surface chemical composition. Journal of Alloys and Compounds, 893, 162304.

[14] Salim, K., & Amroun, M. N. (2022). Study of the effects of annealing temperature on the properties of ZnO thin films grown by spray pyrolysis technique for photovoltaic applications. Int. J. Thin. Film. Sci. Tec, 11(1), 19–28.

[15] Salim, K., & Azzaoui, W. (2023). Physical properties of spray pyrolysed ZnO thin films obtained from nitrate, acetate and chloride precursors: Comparative study for Solar Cell Applications. Revista Mexicana de Fisica, 69(3).

[16] Samadi, M., Zirak, M., Naseri, A., Khorashadizade, E., & Moshfegh, A. Z. (2016). Recent progress on doped ZnO nanostructures for visible-light photocatalysis. Thin Solid Films, 605, 2–19.

[17] Shahzad, S., Javed, S., & Usman, M. (2021). A Review on Synthesis and Optoelectronic Applications of Nanostructured ZnO. In Frontiers in Materials (Vol. 8). Frontiers Media S.A.

[18] Xuan, J., Zhao, G., Sun, M., Jia, F., Wang, X., Zhou, T., Yin, G., & Liu, B. (2020). Low-temperature operating ZnO-based NO2sensors: A review. In RSC Advances (Vol. 10, Issue 65, pp. 39786–39807). Royal Society of Chemistry.

[19] Zhang, C., Zhao, D., Gu, D., Kim, H., Ling, T., Wu, Y. R., & Guo, L. J. (2014). An ultrathin, smooth, and low-loss Al-doped Ag film and its application as a transparent electrode in organic photovoltaics.

[20] Atul Sarojwal and Akriti Garg 2024. Enhancing Solar PV Array Output and Efficiency through IoT-Based Modern Techniques. International Journal of Innovations in Science, Engineering And Management. 3, 2 (Dec. 2024), 214–222. DOI:https://doi.org/10.69968/ijisem.2024v3si2214-222.